International Journal of Medical, Medicine and Health Sciences
ISSN: 2517-9969
Vol:7, No:5, 2013

Hemodynamic Characteristics in the Human Carotid Artery Model Induced by Blood-Arterial Wall Interactions

Taewon Seo

***Abstract*—**The characteristics of physiological blood flow in human carotid arterial bifurcation model have been numerically studied using a fully coupled fluid-structure interaction (FSI) analysis. This computational model with the fluid-structure interaction is constructed to investigate the flow characteristics and wall shear stress in the carotid artery. As the flow begins to decelerate after the peak flow, a large recirculation zone develops at the non-divider wall of both internal carotid artery (ICA) and external carotid artery (ECA) in FSI model due to the elastic energy stored in the expanding compliant wall. The calculated difference in wall shear stress (WSS) in both Non-FSI and FSI models is a range of between 5 and 11% at the mean WSS. The low WSS corresponds to regions of carotid artery that are more susceptible to atherosclerosis.

***Keywords*—**Carotid artery, Fluid-structure interaction, Hemodynamics, Wall shear stress.

I. Introduction

IN the common carotid and the internal carotid arteries, both transient ischemic attack and stroke can occur from thrombotic and embolic complications of atherosclerosis. Atherosclerotic plaques in carotid artery may develop a high level of stenosis that causes the remodeling of arterial wall. Understanding how atherosclerotic plaque initiates, grows to occlude the lumen, ruptures or remains stable will allow clinicians to predict how the plaque develops. Since plaque rupture often tends to be clinically silent until the time of rupture, the exact mechanism of plaque rupture remains unknown. Many *in vivo*, *in vitro* and numerical experiments have been performed to understand the mechanism of atherosclerosis [1]-[3]. As a result, many theories on the atherosclerosis development including hemodynamic effect were built.

As atherosclerosis develops, arteries undergoing early and late stage of plaques as well as large deformations are affected by the stress distribution in the arterial wall [4], [5]. To estimate the level of stress on the plaque accurately, the fluid-structure interaction (FSI) method is needed to consider the hemodynamic factors surrounding the plaque region and the corresponding arterial wall deformation caused by blood flow. There are numerous FSI studies that assume either simple or complex geometry models. For example, Tang et al. [6] generated the simple elastic stenotic tubes simulating blood flow in stenotic carotid arteries. They observed complex flow patterns and high shear stresses at the throat of the stenosis in the case of compressive stresses inside the tube. Similarly Powell [7] measured the tube law for bovine carotid artery and studied the effects of severity of stenosis. The results of the research showed that the tube wall collapsed under physiological conditions. Buchanan [8] studied rheological effects on pulsatile laminar flow through an axisymmetric stenosed tube and found that they could affect wall shear stress quantities. Buriev and Seo [9] investigated shear stresses along the wall, velocity field, wall motion and recirculation zones in the different type of constriction of the blood vessel.

Recently, studies [5], [9], [10] have investigated the flow field in the carotid artery considering fluid-structure interaction and the comparison between Newtonian and Non-Newtonian fluid. Fan et al. [10] suggest that the flow behaviors obtained by the Casson model had no difference when compared with the flow characterizations obtained by the Newtonian model. However, the difference between Newtonian and Non-Newtonian simulations mainly appears in the region of low shear rate and flow recirculation zones.

The main purposes of this study are to investigate the hemodynamic characteristics on the distribution of wall shear stress and flow patterns induced by the arterial wall deformation. It is also studied the comparison of the results between rigid wall model and FSI model.

II. Formulation of Problems

A. Geometric Model of Carotid Artery

The basic geometrical data of model in Fig. 1 is derived from Shaik et al. [5]. The physiological waveform of mean inlet velocity is applied from Fig. 2. The model geometry is generated using Pro-E V5 (PTC). The model consists of the common carotid artery with a diameter D=7.2mm and the bifurcation ($\theta=60^o$) into the internal and external carotid artery. The thickness of the artery wall is assumed to measure 0.2mm. The bifurcation angle, θ, is defined as the angle between the centerlines of internal and external carotid arteries. The model is fully three-dimensional and the cross-sections of the carotid arteries are circular.

B. Blood Flow Modeling

The blood in carotid artery is assumed to be incompressible, laminar and Newtonian governed by the Navier-Stokes equations, while the wall is isotropic and elastic. The continuity equation can be expressed as

T.W Seo is with the Andong National University, Andong, 760-749Korea (phone: 82-54-820-5756; fax: 82-54-820-5044; e-mail: dongjin@ anu.ac.kr).

$$\nabla \cdot u_i = 0 \tag{1}$$

where u_i represents the velocity field with (u, v, w), respectively.

The momentum equations are:

$$\frac{\partial u_i}{\partial t} + u_j \frac{\partial u_i}{\partial x_j} = -\frac{1}{\rho_f}\frac{\partial p}{\partial x_i} + \frac{\partial}{\partial x_j}\left[\frac{\mu}{\rho_f}\left(\frac{\partial u_i}{\partial x_j} + \frac{\partial u_j}{\partial x_i}\right)\right] \tag{2}$$

where x_i is (x, y, z), ρ_f is the blood density and μ is the dynamic viscosity.

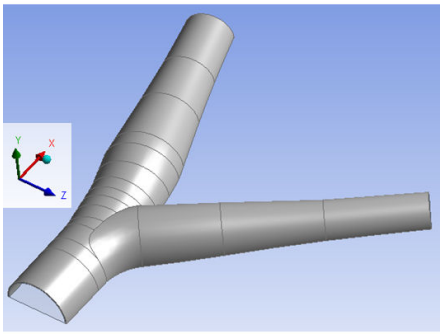

Fig. 1 The carotid artery geometry with arterial thickness

The stress tensor in the Cartesian tensor notation is defined below:

$$\begin{cases} \sigma_{ij} = -p\delta_{ij} + \tau_{ij} \\ \tau_{ij} = 2\mu\varepsilon_{ij} \\ \varepsilon_{ij} = \frac{1}{2}\left(\frac{\partial u_i}{\partial x_j} + \frac{\partial u_j}{\partial x_i}\right) \end{cases} \tag{3}$$

where δ_{ij} is the Kronecker delta, τ_{ij} are the components of the shear stress tensor, ε_{ij} are the components of rate of deformation tensor, μ is the dynamic viscosity of the fluid.

C. Arterial Wall Modeling

The arterial wall is considered to be isotropic and elastic with Young's modulus E=0.5MPa, Poisson's ratio ν = 0.45 and density of blood vessel wall ρ_s = 1,120(kg/m^3). The thickness of the blood vessel wall is uniform at 0.2mm in normal region.

The motion of an elastic vessel wall is mathematically described by the equation shown below:

$$\rho_s \frac{\partial^2 d_i}{\partial t^2} = \frac{\partial \sigma_{ij}}{\partial x_j} \tag{4}$$

where ρ_s is the vessel wall density, d_i are the components of the wall displacements and σ_{ij} are the components of the wall stress tensor. The stress tensor σ_{ij} is obtained from the constitutive equation of the material, and it can be expressed like a Hookean elastic wall as:

$$\sigma_{ij} = \lambda_L e_{kk}\delta_{ij} + 2\mu_L e_{ij} \tag{5}$$

where λ_L and μ_L ate the Lame constants and $e_{ij}$are the components of the strain tensor in the solid.

The conditions of displacement compatibility and traction equilibrium along the fluid-structure interface are satisfied:

- Displacement Compatibility

$$\vec{d}_f = \vec{d}_s \tag{6}$$

- Traction Equilibrium

$$\vec{f}_f = \vec{f}_s \tag{7}$$

where $\vec{d}$ and $\vec{f}$ are displacement and tractions and the subscripts *f* and *s* stand for fluid and solid respectively

D. Boundary Conditions and Numerical Method

The physiological flow patterns are specified by the temporal waveform in the CCA, ICA and ECA as shown in Fig. 2. In this study the mean velocity and the maximum velocity at CCA in Fig. 2 are 0.075m/s and 0.142m/s, respectively. The Reynolds numbers based on CCA diameter corresponding at the peak systolic and mean flows are 307 and 158.9. The period of cardiac cycle is 1 second. The Womersley number is a dimensionless parameter used to characterize pulsatile flow in artery. The Womersley number, which is defined as$\alpha = \frac{D}{2}\sqrt{\frac{\rho\omega}{\mu}}$, is calculated to be 1.97 in this study.

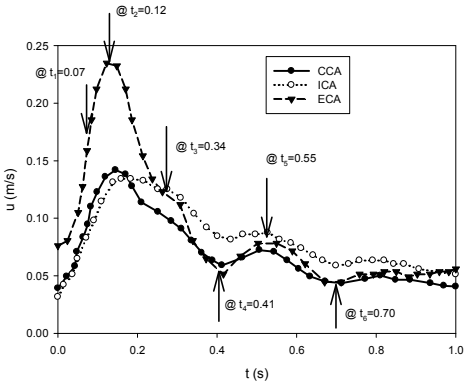

Fig. 2 The physiological flow profiles are specified by the temporal waveform in the CCA, ICA and ECA

The inlet velocity initially accelerates and reaches a maximum at t = 0.12. After this point the velocity magnitude begins to decrease and drops to 0.059m/sec at t = 0.41. In this study the results can be compared six different times corresponding to the conditions of accelerating point (@ t=0.07), peak systole (@ t=0.12), decelerating point (@ t=0.34) and local minimum and maximum velocities (@ t=0.41, 0.55 and 0.70) on each waveform.

In the simulation, the time varying temporal physiological waveform of velocity was specified at the inlet of the CCA as shown in Fig. 2. The velocity profile is applied at the inlet

boundary. At the outlet, the opening pressure boundary conditions were applied to the ICA to the ECA outlet and mesh motion is adjusted by the arterial wall motion. The interface between blood and arterial wall are considered as elastic, and no-slip boundary conditions are imposed on the walls. In the symmetry plane the mesh motion is set to be unspecified.

Before conducting the simulations, grid sensitivity tests were performed at uniform steady flow, u=0.142m/s. Five different mesh densities were used for mesh sensitivity test from 231,401 to 1,844,451 tetrahedral cells. The adopted number of computational grid cells was 1,314,097 tetrahedral cells for model.

The governing equations were solved using two ANSYS Multi-field solvers for ANSYS Structure Mechanics for arterial wall deformation and ANSYS CFX for corresponding blood flow. In these two field solvers the deformation of FSI interface is calculated during structure simulation and the corresponding fluid mesh need to be regenerated and flow field to be calculated after structure simulation at each step. The force collected from ANSYS CFX loads in FSI interface to structure deformation. These iterations continue until physical field solutions meet the convergence criteria.

All simulations in the study were performed using either Intel Xeon 2.67GHz (48GB of RAM) or Intel i7-26003.4GHz personal computer running 64bit Windows 7. In the pulsatile simulations, a total of 86 uniform time steps per cardiac cycle were used. The simulation was carried out over four cardiac cycles. The convergence for each time step in the simulation was based on the residual in continuity falling below a prescribed value (typically 10^{-5}). Under those conditions, differences in velocities among successive cycles were smaller than 1%. All solutions presented have been verified to be mesh-independent – increasing the mesh density yields velocities that are within 1% of those shown here.

III. Results and Discussion

A. Flow Phenomena

Fig. 3 illustrates the comparison of the velocity contours in the symmetry plane between Non-FSI and FSI simulations at t_1, t_2, t_3 and t_6. Although the flow characteristics show similar behaviors in both Non-FSI and FSI simulations, the effect of arterial wall motions appears clearly. While the arterial wall is contracted in the systolic period (see Figs. 3 (b) and (d)), flow velocity is increased by passing through the narrowed cross-section. As a result, it can be concluded that the recirculation region near the outer walls in ICA and ECA is formed larger in FSI simulation than in Non-FSI simulation. At the peak of systole no flow separation is found. Whereas in the diastolic period the arterial wall is expanded, it can be seen that the flow behaviors in both cases are similar as shown in Figs. 3 (e)~(h). As shown in these figures, the extent of flow separation is highly dependent on the flow divider angle. This affects the particle residence time such as platelet or leukocyte. It can be predicted that the long particle residence time will increase the deposition of platelets and the transport of monocytes into the endothelium to generate the foam cells derived from both macrophages and smooth muscle.

As the flow begins to decelerate after the peak flow, a large recirculation zone develops at the non-divider wall of both ICA and ECA in FSI model due to the elastic energy stored in the expanding compliant wall. As a result, the flow phenomenon becomes more complicated and skews strongly toward the inner wall due to the centrifugal forces.

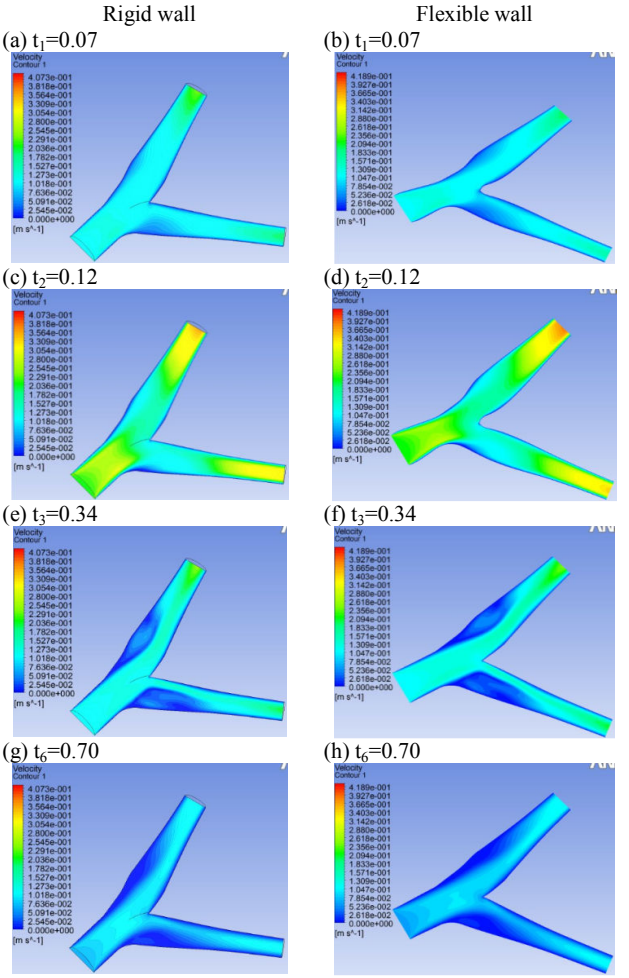

Fig. 3 The comparisons of the velocity contours in the symmetry plane between Non-FSI and FSI simulations

As shown in Fig. 3 the peak velocity in the carotid sinus leans toward the divider wall due to the effect of the bifurcation. The strong flows at t_1 and t_2 were observed near the divider wall, while the large reversed flows were occurred at the non-divider wall at t_3 and t_6.

Fig. 4 shows the comparison of the streamlines in the symmetry plane between Non-FSI and FSI simulations at t_1, t_2, t_3 and t_6. As shown in Figs. 4 (a)~(d) the flow accelerates during the systolic period, and has a strong momentum in both cases. Thus it can be seen that the blood flow in downstream direction looks naturally flowing streams. During the diastolic period in Figs. 4 (e)~(h) the flow characteristics in the Non-FSI analysis

looks more complicated than in the FSI analysis. It can be seen that the complex secondary flow occurs in the non-divider wall in Non-FSI case, while the secondary flow pattern appears weak in FSI case as shown in Figs. 4 (e)~(h). As a result, it can be inferred that the differences due to the effect of the artery deformation lead to the hardening of the vascular wall, as well as the complexity in the flow. In both Non-FSI and FSI models, as the flow continues to decelerate, the vortices increase in size and move downstream during the physiological cycle.

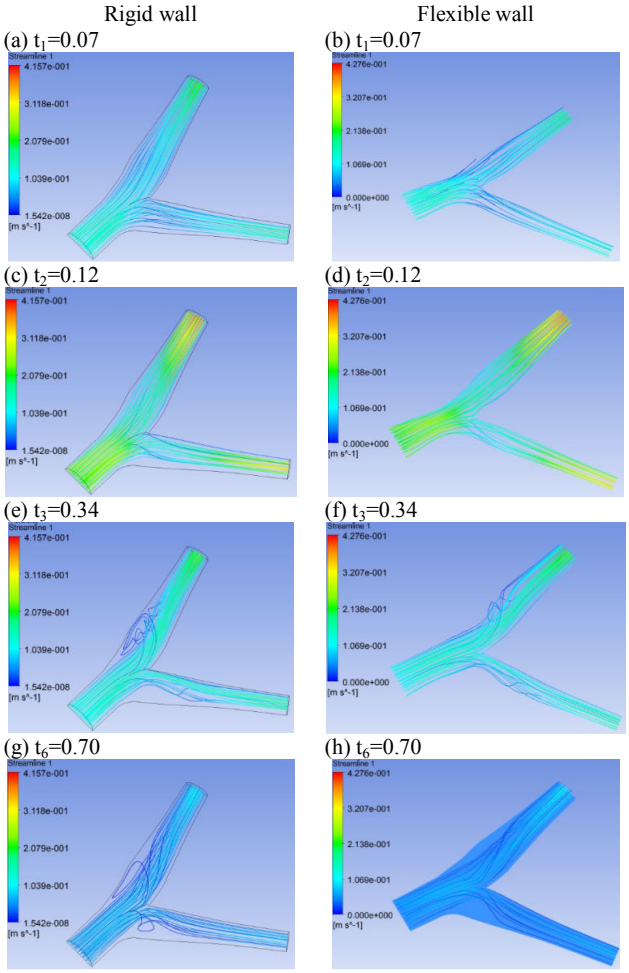

Fig. 4 The comparisons of streamlines in the symmetry plane between Non-FSI and FSI simulations

B. Wall Shear Stress

Fig. 5 represents the comparison of the WSS in the interface of blood and arterial wall between Non-FSI and FSI simulations at t_1, t_2, t_3 and t_6. In the contour the maximum WSS was intentionally fixed at a value of 1pa because many references have been reported that the atherosclerosis is likely to occur at areas of low WSS.

It is noted that the WSS at the apex is the highest at a location where the flow splits between the ICA and ECA, while the WSS in the non-divider region is the lowest. The WSS drops across the sinus in the cases of both Non-FSI and FSI during the decelerating period in cycle.

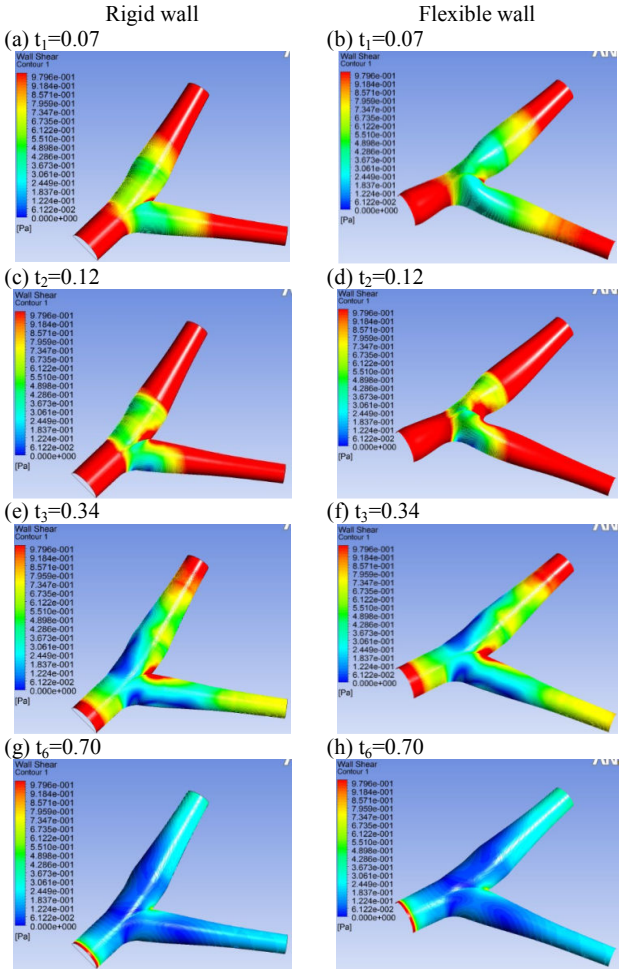

Fig. 5 The comparisons of the wall shear stresses in the interface between Non-FSI and FSI simulations

Fig. 6 illustrates the comparison of the WSS along the inner and outer walls in the ICA or ECA between Non-FSI and FSI simulations at t_2, t_4 and t_5. At the peak flow, the value of the mean WSS for the cycle in FSI model along the inner wall in ECA is 1.68pa. When comparing the mean WSS between Non-FSI and FSI models, the vascular wall of WSS is 8.2% larger in FSI model than in Non-FSI model. However, the vascular wall at t_4 and t_5 is 5.5~6.6% less in FSI model than in Non-FSI model. Along the ICA inner wall the vascular wall at t_2 is 7.83% larger WSS in FSI model than in Non-FSI model, while the vascular wall at t_4 and t_5 is 3~5.8% less WSS in FSI model than in Non-FSI model

Along the ECA outer wall the vascular wall at t_2 is 8.78% larger WSS in FSI model than in Non-FSI model, while the vascular wall at t_4 and t_5 is 11~8.6% less WSS in FSI model than in Non-FSI model. Along the ICA outer wall the vascular wall at t_2 is 10.1% larger WSS in FSI model than in Non-FSI model, while the vascular wall at t_4 and t_5 is 0.5~11.1% less WSS in FSI model than in Non-FSI model.

(a) WSS along the ECA inner wall

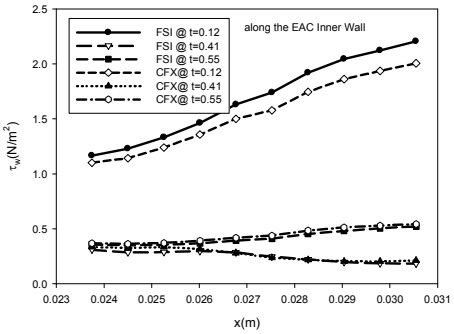

(b) WSS along the ECA outer wall

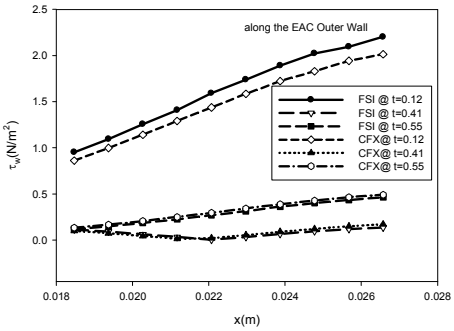

(c) WSS along the ICA inner wall

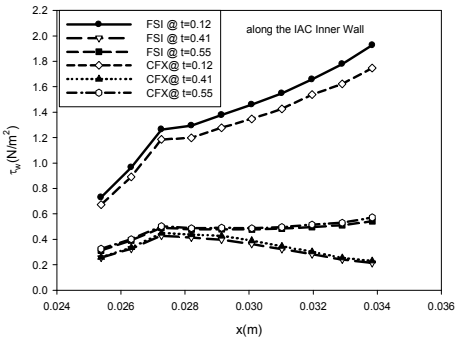

(d) WSS along the ICA outer wall

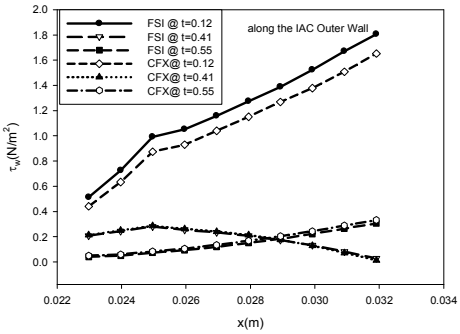

Fig. 6 The comparisons of the wall shear stresses along the inner and outer wall of ICA and ECA

IV. CONCLUSIONS

This study aims to understand the hemodynamic characteristics in the carotid bifurcation models under physiological flow condition. The results were compared to the flow characteristics and WSS in Non-FSI and FSI models.

The main findings of this study can be summarized as follows:

1. The comparison of calculated results for Non-FSI and FSI models showed that a large recirculation zone develops at the non-divider wall of both ICA and ECA in FSI model due to the elastic energy stored in the expanding compliant wall.
2. The differences due to the effect of the artery deformation lead to the hardening of the vascular wall, which consequently causes the blood flow to be more complex.
3. The WSS at the apex is the highest at a location where the flow splits to the ICA and ECA, while the WSS in the non-divider region is the lowest.

ACKNOWLEDGMENT

This research was supported by Basic Science Research Program through the National Research Foundation of Korea(NRF) funded by the Ministry of Education, Science and Technology(Grant Number: 20110026562) and byAndong National University (Dec. 2011).

REFERENCES

[1] P.J. Blanco, M.R. Pivello, R. A. Feijoo, & S.Urquiza, Sensitivity of blood flow at the carotid artery to the heart inflow boundary condition, *3rd International Congress on Comput. Bioeng*., Isla de Maragarita, Venezuela(2007) 1-6.

[2] S.Z. Zhao, X.Y. Xu, A.D. Hughes, S.A. Thom, A.V. Stanton, B. Ariff, & Q. Long, Blood flow and vessel mechanics in a physiologically realistic model of a human carotid arterial bifurcation,*J. of Biomech,* 33 (2000)975-984.

[3] N. A., Buchmann& M.C. Jermy, Blood flow measurements in idealized and patient specific models of the human carotid artery, *14th Int. Symp. On Applications of Laser Techniques to Fluid Mechanics*, Lisbon, Portugal (2008) 1-11.

[4] S.W. Lee, L. Antiga, D. Spence & D.A. Steinman, Geometry of the carotid bifurcation predicts its exposure to disturbed flow, *Stroke AHAJ*, 39 (2008)2341-2347.

[5] E. Shaik, K.A. Hoffmann & J.F. Dietiker, Numerical flow simulations of blood in arteries, *4th AIAA Aerospace Science Meeting and Exhibit*, Reno, Nevada, USA (2006)294-307.

[6] D. Tang, J. Yang, C. Yang & D. N. Ku, Experiment – based numerical simulation of unsteady viscous flow in Stenotic Elastic Tubes, *J. Biomech. Eng*., 121 (2001) 299-320.

[7] B. E. Powell Experimental measurements of Flow through stenotic collapsible tubes, M. S. Thesis, Georgia Inst. of Tech. (1991).

[8] Jr., J. R. Buchanan, C. Kleinstreuer& J. K. Comer, Rheological Effects on Pulsatile Hemodynamic in a Stenosed Tube, *Compute. Fluids*, 29 (2000) 695–724.

[9] B.Buriev& T.W. Seo, Fluid-Structure Interactions of Physiological Flow in Stenosed Artery, *J. Korea-Australia Rheology*, 21 (2009) 39-46.

[10] Y. Fan, W. Jiang, Y. Zou, J. Li,J.Chen& X. Deng, Numerical simulation of pulsatile non-Newtonian flow in the carotid artery bifurcation, *ActaMech Sin*, 25 (2009)249-255.

TaewonSeowas born in Seoul, Korea at Oct. 13, 1958. The author graduated from Ajou University, Korea in Mechanical Engineering in 1982. He received a M.S. degree in mechanical Engineering from University of Detroit in 1988, Detroit, MI, and the PhD degree in Mechanical Engineering from Louisiana State University in 1993, Baton Rouge, LA, USA.

He served in Korean army as the second lieutenant for six months. He worked at R & D center of Korea Heavy Industries Ltd. as the Senior Researcher from Feb. 1994 to Feb. 1996. He joined the Andong National University in March 1996. Prof. Seo visited the Department of Hydraulics of Tsinghua University, Beijing, China in Jan., 1998 and the Institute of Fluid mechanics at Erlangen University, Erlangen, Germany in June, 2001 as the visiting scholar. He had a sabbatical year in 2002 at Department of Aeronautical and Mechanical Engineering in University of California, Davis, USA. Previous research interests of Prof. Seo were the flow control and management as well as the two-phase particulate flows. The current research interest is the bio-fluid mechanics.

Prof. Seo works at the Department of Mechanical and Automotive Engineering in Andong National University, Korea. He is member of KSME and Korean Society of Rheology.